HHS Public Access

Author manuscript

Aquat Toxicol. Author manuscript; available in PMC 2017 August 01.

Published in final edited form as:

Aquat Toxicol. 2016 August ; 177: 22–32. doi:10.1016/j.aquatox.2016.05.005.

Chronic exposure of tilapia (*Oreochromis niloticus*) to iron oxide nanoparticles: Effects of particle morphology on accumulation, elimination, hematology and immune responses

Mehmet Ates[a], **Veysel Demir**[b], **Zikri Arslan**[c,*], **Hasan Kaya**[d], **Sevdan Yılmaz**[d], and **Mustafa Camas**[a]

[a]Department of Bioengineering, Tunceli University, Faculty of Engineering, Tunceli, 62000, Turkey

[b]Tunceli University, Faculty of Engineering, Department of Environmental Engineering, Tunceli, 62000, Turkey

[c]Department of Biochemistry and Chemistry, Jackson State University, Jackson, MS 39217, USA

[d]Faculty of Marine Sciences and Technology, Canakkale Onsekiz Mart University, Canakkale, 17100, Turkey

Abstract

Effects of chronic exposure to alpha and gamma iron oxide nanoparticles (α-Fe_2O_3 and γ-Fe_2O_3 NPs) were investigated through exposure of tilapia (*Oreochromis niloticus*) to 0.1, 0.5 and 1.0 mg/L (9.2×10^{-4}, 4.6×10^{-3} and 9.2×10^{-3} mM) aqueous suspensions for 60 days. Fish were then transferred to NP-free freshwater and allowed to eliminate ingested NPs for 30 days. The organs, including gills, liver, kidney, intestine, brain, spleen, and muscle tissue of the fish were analyzed to determine the accumulation, physiological distribution and elimination of the Fe_2O_3 NPs. Largest accumulation occurred in spleen followed by intestine, kidney, liver, gills, brain and muscle tissue. Fish exposed to γ-Fe_2O_3 NPs possessed significantly higher Fe in all organs. Accumulation in spleen was fast and independent of NP concentration reaching to maximum levels by the end of the first sampling period (30^{th} day). Dissolved Fe levels in water were very negligible ranging at 4–6 μg/L for α-Fe_2O_3 and 17–21 μg/L for γ-Fe_2O_3 NPs (for 1 mg/L suspensions). Despite that, Fe levels in gills and brain reflect more dissolved Fe accumulation from metastable γ-Fe_2O_3 polymorph. Ingested NPs cleared from the organs completely within 30-day elimination period, except the liver and spleen. Liver contained about 31% of α- and 46% of γ-Fe_2O_3, while spleen retained about 62% of α- and 35% of the γ-polymorph. No significant disturbances were observed in hematological parameters, including hemoglobin, hematocrit, red blood cell and white blood cell counts ($p > 0.05$). Serum glucose (GLU) levels decreased in treatments exposed to 1.0 mg/L of γ-Fe_2O_3 NPs at day 30 ($p < 0.05$). In contrast, GLU levels increased during the elimination period for 1.0 mg/L α-Fe_2O_3 NPs treatments ($p < 0.05$). Transient increases occurred in glutamic oxaloacetic transaminase (GOT), glutamic pyruvic transaminase (GPT), and lactate dehydrogenase (LDH). Serum Fe levels did not change during exposure ($p > 0.05$), but increased significantly within elimination period due to mobilization of ingested NPs from liver and spleen to blood. Though respiratory burst activity was not affected ($p > 0.05$), lysozyme activity (LA) was

*Corresponding author. Tel. +1 601 979 2072; fax: +1 601 979 3476.

suppressed suggesting an immunosuppressive effects from both Fe_2O_3 NPs ($p < 0.05$). In contrast, myeloperoxidase (MPO) levels increased significantly in treatments exposed to α-Fe_2O_3 NPs ($p < 0.05$), and the effect from γ-polymorph was marginal ($p \geq 0.05$). The results indicate that morphological differences of Fe_2O_3 NPs could induce differential uptake, assimilation and immunotoxic effects on *O. niloticus* under chronic exposure.

Keywords

Iron oxide nanoparticles; Morphology; Accumulation; Elimination; Hematology; Immune parameters; Tilapia (*Oreochromis niloticus*)

1. Introduction

Nanotechnology industry is among the most rapidly developing sectors because of widespread use of products composed of or containing nanomaterials in biomedical research, electronics and entertainment industries, energy generation and storage, agriculture, food, environmental health and hygiene industries. Despite the fascinating properties of nanomaterials, side effects or impact on human life and the environment are largely unknown (Dreher, 2004, Sanchez et al., 2011). Moreover, the concerns about the potential adverse effects of engineered nanomaterials continue to be more prominent as new materials manufactured for consumer and environmental applications are released increasingly to the aquatic ecosystems (Scown et al., 2010; Sun et al., 2014).

Iron oxide nanoparticles (NPs) possess unique properties for biomedical, technological and environmental applications. They are considered to be relatively well-tolerated in the human body and are widely used in drug delivery, magnetic detection, hyperthermia and magnetic resonance imaging (MRI) (Gupta and Gupta, 2005; Ito et al., 2005; Yu et al., 2008. In MRI, there are used as contrast agents and afford longer imaging capability owing to their longer half-life (Winer et al., 2011). Besides biomedical applications, iron oxide NPs have found applications in terabit magnetic storage and biosensors (Huber 2005), groundwater treatment (Shipley et al. 2011), photocatalytic processes (Bakardjiva et al., 2007; Khedr et al., 2009), and environmental remediation and removal of metallic and organic pollutants from water (Karn et al., 2009; Sanchez et al. 2011; Grover et al. 2012). The increasing commercial use of iron oxide NPs for environmental applications will consequently lead to release of large quantities to the environment and aquatic ecosystems that could pose risks to aquatic organisms. Most studies concerning toxicity of iron oxide NPs have focused on *in vitro* toxicity because of their intriguing medicinal properties (Soenen and De Cuyper, 2010; Mahmoudi et al. 2011; Diana et al. 2013; Ebrahiminezhad et al., 2015; Shen et al., 2015). In general, dose-dependent toxic effects were observed from iron oxide NPs. The mechanism of cellular damage was attributed to reduction of iron resulting in formation of reactive oxygen species (ROS) that cause oxidative stress through lipid peroxidation within cells (Mahmoudi et al. 2011; Diana et al. 2013; Ebrahiminezhad et al., 2015). The effects also varied with particle size; agglomeration to larger particles was reported to decrease the cytotoxicity of iron oxide NPs (Ebrahiminezhad et al., 2015).

The most commonly manufactured or synthesized forms of iron oxide NPs include magnetite (Fe_3O_4) and hematite (Fe_2O_3) that are also the major forms found in the environment originating from anthropogenic emissions and volcanic eruptions. Though aquatic ecosystems are the primary repositories for these NPs, their fate, transport/transformations in aquatic ecosystems and food web, and potential impact on aquatic microorganisms and fish and are not fully understood. Bombin et al. (2015) have reported that treatment with Fe_2O_3 NPs affected adversely reproductive capacity of *Arabidopsis thaliana*. Pollen viability increased up to 6% with up 11% reduction in seedling yield at 3 mg/L levels, whereas exposure to 25 mg/L Fe_2O_3 NPs caused significant reduction in root length besides reduced seedling. Fe_2O_3 NPs decreased the snout-vent length of *Xenopus laevis* tadpoles at 10 mg/L level, and caused significant reduction in total body length at 1000 mg/L levels (Nations et al., 2011). Exposure to suspensions of α-Fe_2O_3 NPs caused significant mortality, hatching delay and malformation in zebrafish *(Danio rerio)* embryos at and above 10 mg/L levels (Zhu et al., 2012). More recently, Zhang et al. (2015) reported that Fe_2O_3 and Fe_3O_4 NPs accumulated heavily in adult zebrafish *(Danio rerio)* with total Fe content of as high as 1.32 and 1.25 mg/g, respectively during 28 days exposure. Guts were filled with aggregates of the NPs, but all cleared from the body within 24 days. With that, it was suggested that ingested NPs did not bioaccumulate in tissues rather they were stored or adsorbed through the gastrointestinal tract.

The current state of the knowledge about the biological and ecological safety of iron oxide NPs indicates that these NPs are not totally benign. Toxic effects vary with species as well as exposure regimes suggesting that exposure to iron oxide NPs could induce harmful effects on aquatic organisms necessitating extensive studies to understand their environmental and aquatic impacts. In this study, we investigated long-term effects of iron oxide (Fe_2O_3) NPs using tilapia (*Oreochromis niloticus*), an important freshwater species of aquatic food chain. Fish were exposed to 0.1, 0.5 and 1.0 mg/L (9.2×10^{-4}, 4.6×10^{-3} and 9.2×10^{-3} mM) aqueous suspensions of α-Fe_2O_3 and γ-Fe_2O_3 NPs for a period of 30 and 60 days, and then transferred into NP-free water and allowed to cleanse ingested NPs for another 30 days. The objective of the study was to investigate the effects of morphological differences between the Fe_2O_3 NPs on accumulation, elimination and potential adverse effects of exposure on *O. niloticus*. Blood parameters were scrutinized during the course of exposure and elimination periods to elucidate the impact of chronic exposure to Fe_2O_3 on hematological and immunological system of the fish.

2. Materials and methods

2.1. Nanoparticles and experimental animals

Alpha iron oxide (α-Fe_2O_3 20-40 nm) and gamma iron oxide (γ-Fe_2O_3 20-40 nm) NPs were procured from Sigma Aldrich Corporation, St. Louis, MO, USA, and were stored under moisture-free conditions until implementation of the experiments. A total of 315 tilapia (*Oreochromis niloticus*) were used in the study. Fish with an average length of 12 ± 1 cm and weight of 30 ± 3 g were obtained from Çukurova University, Aquaculture Department, (Adana, Turkey). The fish were acclimated to ambient conditions for 15 days in resettled tap water in stock aquaria. The fish were fed with fish food during the adaptation period (protein

ratio of 35% and 10% fat). Feeding was interrupted 24 h before the start of the experiment. Before initiating exposure experiments, approval was obtained from the Ethics Committee Approval for Animal Experiments of Çanakkale Onsekiz Mart University.

2.2. Preparation of nanoparticle suspensions and characterization

Stock suspensions (10% w/v) were prepared by suspending appropriate amounts of α-Fe_2O_3 and γ-Fe_2O_3 NPs in ultra-pure water. The stock suspensions were vortexed for 20 s for mixing and then were subjected to ultrasounds in ultrasonic bath for 10 min for maximum dispersion. Appropriate volumes were taken from the suspensions and immediately added into exposure aquaria.

Characterization of NPs was carried out with X-Ray Diffraction (XRD), Transmission Electron Microscopy (TEM), and Dynamic Light Scattering (DLS). Crystal structures of the NPs were verified with X-Ray diffractometer (D8 Advanced X-Ray diffractometer, Bruker, Germany) equipped with X-ray tube with a Cu anode (λ=1.54 A°) as the primary x-ray beam source. Approximately 250 mg of α-Fe_2O_3 and γ-Fe_2O_3 NPs were placed separately on the sample holder. XRD patterns were recorded by operating the anode at 2.2 kW. The scanning speed and step were 1° min^{-1} and 0.02°, respectively. Crystal structure was identified with the diffraction pattern and crystallite size was calculated with Scherrer equation.

Particle size and shape of the Fe_2O_3 NPs were characterized with JOEL-1011 TEM instrument providing 0.2 nm grid resolution with 50 to 1×10^6 magnification under 40-100 kV accelerating voltage. For TEM measurement, one drop (ca. 10 μL) of colloidal NP solution was dropped on 50 A° thick carbon-coated copper grids, and left for drying for 24 h to record the TEM image. Mean particle diameter was identified with ImageJ software program for a group100 NPs from randomly taken views. Hydrodynamic sizes of the α-Fe_2O_3 and γ-Fe_2O_3 NPs in their stock solution and exposure medium were determined by DLS (Malvern Nano ZS Zetasizer). Stock solutions were further diluted to reduce concentration (<10 mg/L). A portion of each suspension was subjected to sonication for a few minutes to dismantle aggregations and then placed in clean 1.5 mL cuvettes. Five DLS measurements were taken from the medium for each NP solution. Zeta potentials were measured for same suspensions by placing 1 mL suspension into the cuvette equipped with electrodes.

2.3. Exposure design

Chronic exposure was conducted according to Organization for Economic Cooperation and Development (OECD section 203) test guidelines (OECD, 2004). Three treatments along with a control group (NP-free water) were used. Exposure was conducted in 40-L graduated aquaria (40×20×80 cm) filled with 20 L filtered tap water. The NPs were added from the freshly prepared stock suspensions directly into exposure tanks (20 L) to provide 0.1, 0.5, and 1.0 mg/L (9.2×10^{-4}, 4.6×10^{-3} and 9.2×10^{-3} mM) NP concentrations. All tanks were constantly aerated to maintain the oxygen level. Detailed description of the exposure settings is given in Table 1. In a 90-day long-term regimen, the fish in treatment groups were exposed to 0.1, 0.5, and 1.0 mg/L (9.2×10^{-4}, 4.6×10^{-3} and 9.2×10^{-3} mM) aqueous suspensions of α-Fe_2O_3 and γ-Fe_2O_3 NPs for 60 days. At the end of the exposure, the fish

were removed from the exposure tanks and placed into freshwater tanks with same physical and chemical aqueous conditions of the control group (e.g., NP free tap water) to determine the elimination of the ingested NPs and changes in biochemical indicators for next 30 days.

Exposure was conducted in a semi-static manner in that test water was replaced daily; 60% in the morning and 40% in the evening. In each water replacement, NP concentrations were established to 0.1, 0.5, and 1.0 mg/L (9.2×10^{-4}, 4.6×10^{-3} and 9.2×10^{-3} mM) levels from fresh stock suspensions. No food was given 24 h prior to the experiment to minimize adsorption of NPs on food and fecal material. For ethical reasons, however, fish were fed once every 10 days to avoid aggressive behavior associated with hunger. Feeding was made 1 h min prior to water exchange in the morning. Once all food was consumed, 60% of the water was replenished and NPs were re-dosed to appropriate concentrations. In each feeding, food was consumed rapidly; visually there was not any left-over food or suspending waste before water change. Exposure was performed with 16:8 h daylight:darkness regime at 25 ± 0.5 °C with the following physico-chemical conditions: 5.4 ± 0.2 mg/L dissolved oxygen content; 6.90 ± 0.1 pH; 132 ± 6 mg/L $CaCO_3$ total hardness. Sampling was made at four intervals; before any chemical exposure (day 0), and on the 30th, 60th and 90th day from the start of the experiment. On day 0, 10 fish from stock fish aquaria were taken. On the 30th, 60th, and 90th days, 5 fish from control aquaria and 5 fish from each treatment aquarium (5 fish/aquarium * 21 aquaria = 105 fish) were randomly taken out.

Temperature and dissolved oxygen content were measured daily with YSI 556 multi-probe. The pH of exposure medium was measured daily with a HANNA C 200 (HI 83200) multi-parameter bench photometer. Samples of water were taken from the exposure tanks once every other day to measure hardness with an Optizen POP UV-VIS spectrophotometer. Electrolyte analyses were conducted with a Varian Liberty Sequential ICP-OES. Dissolved Fe levels were also measured from the water samples to rationalize the effects of particle morphology on accumulation and elimination patterns. Of the water samples from exposure tanks, 2 mL were centrifuged for 30 min at 12,000 rpm to remove larger Fe_2O_3 particles and aggregates. Later, 1 mL of the supernatant water was passed through ultra-filtration filters (VWR International) with a molecular cut-off 3,000 Da to separate dissolved Fe ions (Ates et al., 2013). The filter rejects particles greater than 1.3 nm so that the solution passed through would contain only dissolved Fe and other ions. The 1-mL filtrate was diluted/acidified to 2 mL with 10% (v/v) HNO_3. Iron concentrations were measured by ICP-MS (Varian 820 MS, Australia).

2.4. Analysis of tissues for NP accumulation and elimination

The fish collected randomly from controls and treatments were anesthetized with clove oil and dissected. Gills, liver, kidney, intestine, brain, spleen and muscle tissue were collected and washed with ultrapure water. The samples were prepared for instrumental analysis according to methods described previously (Arslan et al., 2011; Ates et al., 2015). About 0.2 to 0.5 g samples (wet weight) were dried in an incubator for 2 days at 100 °C. Afterwards, each sample was weighed and placed into teflon vessels and digested in 4 mL of 50% HNO_3 in the microwave oven. After the completion of mineralization, the digests were diluted to 50 mL with deionized water. The acid HNO_3 concentration was 4% (v/v) in diluted sample

solutions. Spiny Dogfish (*Squalus acanthias)* muscle (DORM-2) and liver (DOLT-3) certified reference material (CRM) obtained from National Research Council of Canada (CNCR, Ottawa, Ontario, Canada) were used for quality control in Fe determination by ICP-MS. The certified concentration of Fe in DORM-2 and DOLT-3 are 142 ± 10 μg/g and 1484 ± 57 μg/g, respectively. About 0.1 g samples of CRMs were digested similarly and analyzed for Fe with ICP-MS (Varian 820 MS, Australia) simultaneously with tissue samples from tilapia. Iron values in the CRMs were between 95% and 105% of the certified values. The ICP-MS instrument was calibrated with aqueous Fe standard solutions (within 0-1.0 μg/mL Fe) that were prepared in 4% (v/v) HNO_3 from 1000 μg/mL Fe stock standard solution (SCP Science, Champlain, NY, USA). Total Fe concentration measured from sample solutions were expressed as the dry-weight basis (μg/g) of tissues.

2.5. Blood sampling and analyses

Three fish from each aquarium in each collection interval were used for blood analyses. After anesthetizing with clove oil, then the area behind the anus fin was cleaned thoroughly with 70% alcohol to prevent the mixing of the mucous membrane into the blood. Blood was drawn immediately with a 5-mL plastic syringe needle through caudal vein without hurting the animal. For hematological analysis, a portion of the blood samples were transferred into tubes contained K_3EDTA. The remaining portion was taken into serum tubes (with gel) and centrifuged for 5 min at 5,000*g*. The resulting serum samples were kept at −80° C for immunological and biochemical analysis.

2.5.1. Hematological analyses—Hematological analyses (hemoglobin, hematocrit, and red blood cell count) were conducted with automatic blood count instrument (Mindray BC 3000 plus). White blood cells (WBC, $10^3/mm^3$) were also counted in blood smears using the indirect method (number of leukocytes in the blood smear X erythrocytes quantified in the counter/7000 erythrocytes in the blood smear) (Yılmaz et al., 2014).

2.5.2. Measurement of innate immune parameters

2.5.2.1. Respiratory burst activity (RBA): Modified Stasiak and Baumann (1996) method was followed for respiratory burst activity of the phagocytes. A volume of 50 μL from the blood samples were placed into 96 well plates coated with 50 μL of poly-l-lysine (Sigma, P4832) solution and incubated at room temperature for 1 h to allow adhesion of cells. Then, the supernatant was removed and the wells were washed three times in Hanks' Balanced Salt Solution (HBSS, Sigma, H6648). After washing, 100 μL of 0.2% NBT in HBSS solution was added and incubated for another 1 h. The cells were then fixed with 100% methanol for 5 min and washed three times with 70% methanol. The plates were air dried and then 60 μL of 2.0 M potassium hydroxide and 70 μL dimethyl sulphoxide were added to each well. The absorbance (OD) was recorded in a micro-plate reader (Thermo Multiskan Go) at 620 nm.

2.5.2.2. Lysozyme activity: Lysozyme activity was determined by the microtiter plate method (Nudo and Catap, 2012) which measures the lysis of a suspension of *Micrococcus luteus* (ATCC 4698) (75 mg/100 mL) of 0.1 M phosphate/citrate buffer with 0.09% NaCl, pH 5.8). A volume of 175 μL of the bacterial suspension was added to 25 μL of each serum sample, and to lysozyme standard (from hen egg white, Sigma, Cat. No L6876; 0–20 μg/mL

of 0.1 M phosphate/citrate buffer with 0.09% NaCl, pH 5.8) in flat-bottom 96-well plates. The plates were incubated for 30 min. The rate of lysis was determined against *M. luteus* blank at 450 nm on a plate reader. Hen egg white lysozyme was used as an external standard. The rate of reduction in absorbance of the samples was converted to lysozyme concentration (μg/mL) using a standard curve.

2.5.2.3. Myeloperoxidase activity: Total myeloperoxidase (MPO) content in blood plasma was measured according to Quade and Roth (1997) with minor modifications. Ten μL serum was diluted with 90 μL of HBSS without Ca^{2+} or Mg^{2+} in 96 well plate. A volume of 35 μL of 0.1 mg/mL 3,3′,5,5′-tetramethylbenzidine dihydrochloride and 0.06% (v/v) fresh hydrogen peroxide were added. After 2 min, 35 μL of 4 M sulphuric acid was added to stop the reaction and the optical density was read at 450 nm in a plate reader.

2.5.3. Blood enzyme, iron and glucose analyses—The serum biochemical analyses, including alkaline phosphatase (ALP), glutamic oxaloacetic transaminase (GOT), glutamic pyruvic transaminase (GPT), lactate dehydrogenase (LDH) and glucose (GLU) were performed with Thermo multiscan Go micro-plate reader using Bioanalytic brand analysis kit. Serum iron (Fe) measurements were carried out by ICP-MS after digesting 0.1 mL of the serum samples in 50% HNO_3.

2.6. Statistical analyses

The statistical analyses were made using SPSS 21.0, and the significance level was considered to be 0.05. Normality of data and homogeneity of variances were checked using Kolmogorove Smirnov and Levene tests, respectively. When appropriate, One-Way ANOVA and Tukey's sub-test were performed. If normality of variances was not met Kruskal Wallis test was performed.

3. Results

3.1. Crystal morphology of Fe_2O_3 NPs

The XRD diffractograms for α-Fe_2O_3 (hematite) NPs (20-40 nm) showed 11 peaks within 20-80° range with the following 2θ (theta) values: 24.2, 33.2, 35.6, 41.03, 49.4, 53.9, 57.7, 62.4, 64.02, 72.06 and 76.39°. The existence of sharp peaks confirmed that α-Fe_2O_3 NPs were highly crystalline and monodisperse without any impurities (Yin et al., 2011). Crystallite size for 2θ=33.2° calculated with Scherrer formula was 28.25 nm. The XRD diffractogram for γ-Fe_2O_3 (maghemite) NPs showed 6 sharp peaks at 2θ: 30.2, 35.5, 43.2, 53.3, 57.2 and 62.7° that were also consistent with previously published values (Guivar et al., 2014). It was highly crystalline (e.g., pure) with crystallite size of 20.5 nm (2θ=35.6°).

3.2. Size distribution and dissolution of Fe_2O_3 NP suspensions

The TEM images obtained from stock suspensions of α-Fe_2O_3 and γ-Fe_2O_3 NPs are shown in Fig. 1. The size of the particles varied between 20 and 90 nm for α-Fe_2O_3 and 40 and 120 nm for γ-Fe_2O_3 NPs. The images revealed that α-Fe_2O_3 NPs contained a mixture of rod, spherical and cubical particles while γ-Fe_2O_3 NPs were mostly of round or spherical particles. The sizes of the NPs were relatively larger than the reported values indicating that

α-Fe_2O_3 and γ-Fe_2O_3 NPs tended to agglomerate though it was marginal in dried suspensions.

The mean hydrodynamic sizes measured by DLS were 426 ± 19 nm for α-Fe_2O_3 and 304 ± 17 nm for γ-Fe_2O_3 NPs. Both NPs possessed negatively charged surfaces. The zeta potentials for freshly prepared aqueous suspensions were measured to be −23.6 ± 1.6 mV and −18.1 ± 1.3 mV for α-Fe_2O_3 and γ-Fe_2O_3 NPs, respectively. ICP-MS analyses showed that α-Fe_2O_3 and γ-Fe_2O_3 NPs were virtually insoluble in exposure medium. Dissolved Fe concentrations measured from 1 mg/L suspensions ranged between 4 and 6 μg/L for α-Fe_2O_3 NPs, and between 17 and 21 μg/L for γ-Fe_2O_3 NPs. In 0.5 mg/L suspensions, Fe levels were proportionately lower. For 0.1 mg/L suspensions, Fe concentrations were less than 1 μg/L and were indistinguishable between α- and γ-polymorphs. It was, however, evident that the metastable γ-Fe_2O_3 polymorph was about 3 to 4 times more soluble than α-Fe_2O_3 polymorph.

3.3. Accumulation and distribution of Fe_2O_3 NPs in organs

Potential organs, including the spleen, intestine, kidney, liver, brain, and muscle tissue were individually assayed by ICP-MS analyses to portray the physiological uptake, distribution, potential bioaccumulation and elimination profiles of α-Fe_2O_3 and γ-Fe_2O_3 NPs reliably under environmentally relevant conditions. The content of Fe measured in the organs is illustrated in Fig. 2. The order of accumulation was spleen > intestine > kidney > liver> gills > brain > and muscle. The highest Fe content was detected in the spleen and intestine (Fig. 2). Compared to controls, Fe levels increased to as high as 850 μg/g and 600 μg/g in the spleen and intestine, respectively. The accumulation in the intestine exhibited a concentration- and time-dependent pattern. On the 60th day, Fe levels in the intestine of groups exposed 1.0 mg/L α-Fe_2O_3 NPs increased twice as much in comparison to that in on the 30th day ($p < 0.05$). γ-Fe_2O_3 NPs did accumulate even more in 60 days, but not as drastically as α-Fe_2O_3 NPs. In contrast to intestine, NPs incorporated into spleen fast and almost insignificantly of time and concentration. The differences in spleen Fe levels among the treatments were marginal ($p \geq 0.05$).

Liver possessed significant accumulation of both α-Fe_2O_3 and γ-Fe_2O_3 NPs, though the Fe levels in the livers of fish exposed to 0.1 and 0.5 mg/L α-Fe_2O_3 NPs did not have any significant increase compared to the controls in 30 days ($p \geq 0.05$). Iron levels in the liver increased with NP concentration and exposure time, especially for 60-day exposure ($p < 0.05$). Further, groups exposed to γ-Fe_2O_3 NPs had significantly higher Fe levels than those exposed to α-Fe_2O_3 NPs within same concentration regime ($p < 0.05$). Exposure also caused significant NP accumulation in the kidneys. In contrast to that in liver, kidneys of fish exposed to α-Fe_2O_3 NPs possessed substantially higher Fe levels on the 30th day than those of γ-Fe_2O_3 NPs ($p < 0.05$) (Fig. 2). Compared with the controls, kidney Fe levels did increase for γ-Fe_2O_3 NPs treatments ($p < 0.05$), but accumulation was much lower than α-Fe_2O_3 NPs. Further, differences between treatments were not significant ($p > 0.05$); kidney Fe levels measured from 0.1 to 1.0 mg/L γ-Fe_2O_3 NPs groups were statistically indistinguishable. On the 60th day of exposure, kidneys of fish exposed to 0.5 and 1.0 mg/L γ-Fe_2O_3 NPs contained elevated levels of Fe as for those exposed to α-Fe_2O_3 NPs ($p <$

0.05), whereas no significant uptake occurred in treatments exposed to 0.1 mg/L γ-Fe_2O_3 NPs ($p > 0.05$).

Gill tissues contained significant levels of Fe within 30-day exposure ($p < 0.05$), except that for 0.1 mg/L γ-Fe_2O_3 NPs for which Fe levels were similar to those of controls ($p > 0.05$). On the 60th day of exposure, there was a marginal increase in gill Fe levels for α-Fe_2O_3 NPs for similar exposure concentrations, while that for γ-Fe_2O_3 was relatively higher ($p \leq 0.05$). Unlike the fluctuation occurred in α-Fe_2O_3 NPs, accumulation of γ-Fe_2O_3 polymorph into gill tissue appeared to be dependent on time and concentration such that on the 60th day of exposure, accumulation from 0.1 mg/L suspensions were also significantly higher compared with the controls ($p < 0.05$). Exposure resulted in significant increase in Fe levels in the brain tissue of treatments ($p < 0.05$). Uptake showed a time- and concentration-dependent increase. Further, the brain tissue of fish exposed to γ-Fe_2O_3 NPs contained higher Fe levels than that expose to α-Fe_2O_3 NPs ($p < 0.05$). Accumulation in the muscle tissue was the lowest among all the tissues though significant variations were detected in muscle Fe levels (Fig. 2). Iron concentrations in α-Fe_2O_3 NPs treatments were not significantly different from those of controls, even for 60-day exposure ($p \geq 0.05$). On the other hand, Fe levels in muscle tissue of fish exposed to 0.5 and 1.0 mg/L suspensions of γ-Fe_2O_3 NPs increased significantly in 30 days ($p < 0.05$) and continued to increase with exposure time (e.g., 60 days).

3.4. Elimination profiles of Fe_2O_3 NPs

The concentration of Fe in the organs decreased significantly at the end of post exposure period when fish were allowed to eliminate the ingested NPs for the next 30-days in freshwater. The Fe levels in the kidney, brain, muscle tissue, and intestine returned to similar levels with those of controls ($p \geq 0.05$). The gills also mostly cleared out the NPs, except the groups exposed to 1.0 mg/L suspensions of γ-Fe_2O_3 NPs. This result may indicate that accumulation on the gill was mainly from surface adsorption rather than chemical incorporation of NPs into gill tissue. The liver Fe levels decreased by 16% and 69%, but were still significantly higher for groups exposed to 0.5 and 1.0 mg/L levels ($p < 0.05$). Similarly, NPs accumulated in the spleen were completely cleared out within 30 days for 0.1 mg/L exposure groups, whereas Fe levels in the spleen of fish exposed to 1.0 mg/L suspensions were still significant ($p <0.05$); about 62% and 35% of accumulated particles remained in the spleen for α-Fe_2O_3 NPs and γ-Fe_2O_3 NPs, respectively.

3.5. Blood parameters

3.5.1. Hematological findings—Hematological findings of the study are presented in Table 2. White cell blood counts (WBC) were similar in all groups during the exposure periods ($p \geq 0.05$), but increased during the recovery period in groups exposed to 1.0 mg/L γ-Fe_2O_3 NPs when compared to the controls ($p < 0.05$). The data for the rest of the hematological parameters; red blood cell count (RBC), hemoglobin (HGB), and hematocrit (HCT) were not different from that of the controls both in exposure and recovery periods ($p \geq 0.05$).

3.5.2. Immunological findings—Respiratory burst activity (RBA), lysozyme and myeloperoxidase activity were measured to determine the effects of α-Fe_2O_3 and γ-Fe_2O_3 NP exposure on the immune system of *O. niloticus*. The results are shown in Fig. 3. RBA levels showed similarities with the controls on 30th day for all concentrations of α-Fe_2O_3 and γ-Fe_2O_3 NPs ($p \geq 0.05$), but there was a significant increase on the 60th day on those exposed to 0.1 mg/L of α-Fe_2O_3 NPs ($p < 0.05$). At the end of the recovery period, all treatments and the controls demonstrated similar results ($p \geq 0.05$).

Lysozyme is a major antimicrobial enzyme possessing antibacterial and anti-inflammatory functions. On the 30th day, no significant suppression was observed on lysozyme activity, except the treatments exposed to 0.1 mg/L α-Fe_2O_3 NPs (Fig. 3). On the 60th day of the exposure, on the other hand, lysozyme levels were significantly lower in all treatments (with the exception of 1.0 mg/L α-Fe_2O_3 NPs group) ($p < 0.05$). At the end of the recovery period (e.g., 90th day), lysozyme levels returned back to normal values as for the controls ($p \geq 0.05$). Myeloperoxidase (MPO) is an oxidative enzyme and extracellular MPO activity provides an estimate of the oxidative stress in inflammatory conditions. On the 30th day of exposure, MPO activity was not significantly different from those of controls (Fig. 3) ($p \geq 0.05$). On the 60th day, an increase was observed in treatments exposed to 0.5 and 1.0 mg/L of α-Fe_2O_3 NPs ($p < 0.05$). Interestingly, MPO activity was higher for 0.1 mg/L of γ-Fe_2O_3 NPs treatment during the recovery phase ($p < 0.05$), while all other treatments showed similar results with the controls ($p \geq 0.05$).

3.5.3. Serum iron, glucose, enzyme analyses—Iron and glucose analyses were conducted on the serum separated from the blood on sampling periods (day 0, 30, 60, and 90). The serum Fe levels were relatively constant throughout the exposure for either Fe_2O_3 NPs and were not different from those of controls (see Fig. 3) ($p \geq 0.05$). During the elimination (90th day) period, serum Fe levels in treatments exposed of 1.0 mg/L suspensions of α-Fe_2O_3 and γ-Fe_2O_3 NPs were significantly higher compared with controls ($p < 0.05$). Serum glucose levels are summarized in Table 3. The variation in glucose values followed a similar pattern with Fe concentrations. No significant changes were detected during the exposure between treatments and controls ($p \geq 0.05$), but glucose levels increased in fish exposed to 1.0 mg/L of α-Fe_2O_3 NPs at the end of the elimination phase ($p < 0$ .05).

The results for blood enzymes scrutinized are summarized in Table 3. Serum Glutamic Pyruvate Transaminase (GPT) activity increased in the group exposed to 0.5 mg/L γ-Fe_2O_3 NPs on the 60th day of the exposure ($p < 0.05$), while no significant changes occurred in other treatments ($p \geq 0.05$). The increase in serum oxaloacetic transaminase (GOT) activity was statistically significant on the 30th day of the experiment for treatments exposed to 0.1 mg/L α-Fe_2O_3 NPs ($p < 0.05$), while an increase was identified on the 60th day of the study in the groups exposed to 0.5 mg/L γ-Fe_2O_3 NPs ($p < 0.05$). Lactate Dehydrogenase (LDH) findings indicated an increase in LDH levels for the fish exposed to 0.5 mg/L γ -Fe_2O_3 NPs on the 60th day ($p < 0.05$), while the LDH levels for other groups were similar to that of the control group ($p \geq 0.05$). Alkaline Phosphatase (ALP) results varied with concentrations and exposure time, yet the differences were not statistically significant ($p \geq 0.05$).

4. Discussion

4.1. Stability of colloidal Fe_2O_3 suspensions

Sizes of the particles from TEM were relatively larger than the reported values; 20 to 90 nm for α-Fe_2O_3 and 40 to 120 nm for γ-Fe_2O_3. In contrast, hydrodynamic sizes were much larger (426 nm for α-Fe_2O_3 and 304 nm γ-Fe_2O_3 NPs) due to greater particle aggregation in water. These results were similar to that reported in other studies (Zhu et al., 2012, Bombin et al., 2015). Indeed, the size of aggregates were significantly smaller than those (1,025 nm for 30 nm nFe_2O_3 NPs) reported by Zhu et al. (2012).

Loss of colloidal NPs from exposure medium via aggregation is a common hurdle in testing the accumulation and toxicity of NPs on aquatic species. In this study, semi-static exposure was implemented for 60 days during which the exposure medium was replenished twice daily by renewing the 60% of water in the morning and 40% in the evening to ensure stability of colloidal particles. Such protocols are commonly used to maintain concentrations of colloidal particles at desired levels (Handy et al., 2012; Zhang et al., 2015), but sedimentation cannot be completely avoided. For instance, Zhang et al. (2015) reported substantial sedimentation for Fe_2O_3 and Fe_3O_4 NPs; Fe levels decreased by about 30% and 78%, respectively, within the first hour. On the other hand, fish and filter-feeders readily ingest NPs suspended in water. Accordingly, total body burden of NPs in aquatic species have correlated with exposure concentrations (Shaw et al., 2012, Hu et al., 2012; Ates et al., 2013; Kaya et al., 2015; Zhang et al., 2015), suggesting that aggregation may not affect the uptake of NPs under semi-static regimens, though toxic symptoms could vary largely due to formation of more benign bulk particles.

4.2. Accumulation and elimination of NPs in intestine, kidney and spleen

Time- and concentration-dependent accumulation was observed in the organs of tilapia. In general, exposure to γ-Fe_2O_3 NPs suspensions resulted in higher accumulation in all organs, except the spleen where α- and γ-Fe_2O_3 polymorphs showed similar levels. Eventually, highest accumulation occurred in the spleen followed by the intestine and kidney. Intestines in fish have shown to possess elevated levels of particles as they are primary repositories for water-borne and food-borne particles (Ramsden et al. 2009; Hao et al., 2013; Boyle et al., 2013a; Ates et al., 2014; Zhang et al., 2015). Indeed, aggregates of Fe_2O_3 NPs were visually noted in tilapia intestines as for the zebrafish (Zhang et al., 2015). Kidney in fish serves in trapping particles from blood. Consequently, Fe levels in the kidney were as high as that in intestine, and increased with exposure time and NP concentration. Additionally, γ-Fe_2O_3 NPs accumulated more than α-Fe_2O_3. Though this could be affected from greater dissolution of γ-Fe_2O_3, it could also indicate size-dependent retention of particles, that is, hydro-dynamically smaller γ-Fe_2O_3 NPs (e.g., 304 nm) were more effectively trapped than larger α-Fe_2O_3 NPs (e.g., 426 nm). This hypothesis could be verified in future with Fe_2O_3 NPs of varying sizes. In case of elimination, both intestine and kidney were cleared out the accumulated particles within 30-day elimination period (see Fig. 2). Zhang et al. (2015) reported that elimination of Fe_2O_3 and Fe_3O_4 NPs followed a first order decay from exposed zebrafish, and all particles were eliminated within 24 days post-exposure.

Spleen in fish is a secondary filtration organ after kidney; particles and other macromolecules are selectively trapped in splenic ellipsoids. In rainbow trout, maximum size of particles that could enter splenic ellipsoids was estimated to be 0.15 to 0.5 μm, and larger particles were partitioned to the kidney (Espenes et al., 1995). In water-borne exposure to bulk and nanoTiO_2, Ti levels were much higher in spleen of rainbow trout than in kidney (Boyle et al., 2013a), but kidney contained about 10-fold higher Ti (ca. 300 μg/g) than spleen in intravenous exposure where aggregation was substantial in the saline blood plasma (Boyle et al., 2013b). Accumulation in spleen was also faster compared with other organs (Ramsden et al., 2009). Similarly, in this study, accumulation of Fe_2O_3 NPs in the spleen of tilapia was much faster than other organs, and was independent of concentration and the polymorph (see Fig. 2). Maximum levels had already been reached at the first sampling time (e.g., 30^{th} day). Apparently, a large fraction of NPs were within the size range to be effectively retained by the spleen tissue (Espenes et al., 1995). Unlike intestine and kidney, the retained particles could not be cleared out of the spleen within 30-day elimination period, especially for groups exposed to 1.0 mg/L suspensions. Likewise, rainbow trout spleen contained notable levels of Ti after two weeks of recovery period (Ramsden et al., 2009). While these effects are in part due to excessive accumulation, they do clearly indicate slow mobilization of NPs from spleen.

4.3. Accumulation and elimination of NPs in liver, gills, brain and muscle tissue

Besides detoxification, liver serves as filtration site like spleen and kidney, and thus has been a target organ of fish exposed to NPs. In most studies, accumulation of NPs in liver was comparable to or lesser than that in kidney, and was dependent on exposure time, and NP concentration and size (i.e., fine NPs accumulated more than coarse NPs) (Boyle et al., 2013a; Ates et al., 2015; Kaya et al. 2015). On the other hand, elimination was slower as in spleen (Ramsden et al., 2009). Our results are consistent with these findings. In addition, this study demonstrates that γ-Fe_2O_3 NPs accumulated to a greater extent in the liver, but cleared out slower than α-Fe_2O_3 NPs. Of the total Fe, 31 and 46% were in the liver at the end of the elimination period for α-Fe_2O_3 and γ-Fe_2O_3 NPs, respectively. These differences could be related with the polymorph of the Fe_2O_3 NPs. Conversely, Fe released from trapped NPs could be assimilated to higher levels and retained longer in the liver as relatively more soluble metastable γ-Fe_2O_3 NPs are solubilized gradually, yet additional studies with different sizes of Fe_2O_3 NPs and other morphologically different NPs are needed to verify this explanation.

Gills possess large surface area and are primary contact point of fish with suspending particles and contaminates in the water. Extensive accumulation from exposure to NPs of Ag, TiO_2, CuO, and ZnO has been reported on the gills of fish (Zhao et al., 2011; Boyle et al., 2013a, 2013b; Hao et al., 2013; Imani et al., 2014; Ates et al., 2015). Because NP aggregates are too large to penetrate into gill tissue, the accumulation is ascribed to adsorption/adhesion of NPs on the gill epithelial surfaces to varying degrees as determined by NP type, concentration and exposure time (Kaya et al., 2015). Cu levels on the gills of juvenile carp, for instance, remained relatively steady while that of Zn steadily increased over 30-day exposure to CuO (Zhao et al., 2011) and ZnO NPs (Hao et al., 2013). ZnO NPs are more soluble than CuO NPs, and thus this difference is likely due to accumulation of

dissolved Zn in the medium (Ates et al., 2013, 2014). In this study, gill Fe levels increased gradually for γ-Fe_2O_3 polymorph, but remained relatively constant for α-Fe_2O_3 NPs. This result is consistent with those of ZnO NPs and indicative of more dissolved Fe accumulation from water for relatively soluble γ-Fe_2O_3 NPs. Furthermore, our results show that metal levels in gills are not solely from physical adsorption of NPs, instead a combination of NP and dissolved metal ion accumulation, and thus gills could be potential organs for tracing the size-, shape- and polymorph-dependent accumulation and toxicities. The elimination of NPs from gills appears to be dependent on NP type and exposure concentration (Ramsden et al., 2009). In this study, tilapia gills mostly cleared out of Fe in 30 days. Residual Fe was not significant compared with the controls, except for 1.0 mg/L γ-Fe_2O_3 group suggesting that longer time was required for complete elimination. Similarly, Zhang et al. (2015) reported that Fe_2O_3 (alpha polymorph) and Fe_3O_4 NPs cleared off of gills of zebrafish within 24 days.

Brain is considered to be immune against NP accumulation with the assumption that NPs are too large to penetrate through the blood-brain barrier (Ates et al., 2014, 2015; Shaw et al., 2012). Yet, metal levels have been found to increase in the brain of fish exposed to NPs. In exposure to ZnO NPs, for instance, Zn levels in the brain of tilapia were significant on the 14^{th} day of exposure (Kaya et al. 2015), while that in juvenile carp increased steadily for 30 days up to 60 μg/g (Zhao et al 2011). On the other hand, cadmium (Cd) levels in brain of zebrafish were only significant after 60 days in CdS NPs exposure (Ladhar et al., 2014). In this study, Fe levels did increase in the brain of tilapia depending on NP concentration, exposure time as well as polymorph. Evidently, exposure to γ-Fe_2O_3 NPs induced consistently higher Fe than that for α-Fe_2O_3 NPs, indicating accumulation of more dissolved Fe from γ-Fe_2O_3 NPs as for the gills. In contrast, exposure to soluble Zn (2.0 mg/L) did not induce any significant Zn accumulation in the brain of juvenile carp within same exposure unlike ZnO NPs (Hao et al., 2013). However, the information provided here and other studies is far from conclusively verifying whether the metal concentrations measured in brain of fish are from dissolved metal ions, internalized NPs or due to the adhesion of NPs on the surface of brain tissue. Additional studies are needed for selectively measuring the intracellular metal levels to verify the accumulation of NPs in the brain.

Iron levels in muscle tissue of tilapia were very low indicating that muscle tissue is not a repository for Fe_2O_3 NPs accumulation. Likewise, exposure to relatively more soluble γ-Fe_2O_3 NPs induced higher Fe in the muscle than α-Fe_2O_3, but the levels were negligible, presumably due to the lack of metal binding proteins in the muscle. At the end of the elimination period, muscle Fe levels returned to the levels of the controls. These results are consistent with exposure of fish to different NPs in previous studies where metal levels in muscle have been the lowest compared with other organs (Zhao et al., 2011; Boyle et al., 2013a; Hao et al., 2013; Kaya et al., 2015).

4.4. Hematological analyses

Disturbances in hematological biomarkers, such as white blood cell (WBC), red blood cell (RBC), hemoglobin (HGB) and hematocrit (HCT) reflect the physiological suffering of the organism under stress conditions (Shaw et al., 2012; Kaya et al., 2014). Suspensions of α-

Fe_2O_3 and γ-Fe_2O_3 examined in this study did not cause any significant disturbances on WBC, RBC, HCT and HGB levels of tilapia. In contrast, α-Fe_2O_3 NPs induced significant hemolytic disturbances on Indian major carp, *Labeo rohita*, at 500 mg/L levels (Remya et al., 2015). In 96-h acute exposure, α-Fe_2O_3 NPs were also found significantly hemolytic to Indian major carp, decreasing HCT and HBG values by 72 and 77% even at 1 mg/L levels (Saravanan et al., 2015). RBC counts did not change in acute exposure (Savaranan et al., 2015), but increased consistently to as high as 237% in exposure to 500 mg/L α-Fe_2O_3 NPs (Remya et al., 2015). This result reflecting the increased oxygen demand or reduced gas-exchange is likely caused by deposition of NPs heavily on the gills under elevated Fe_2O_3 NPs conditions.

4.5. Blood serum analyses

Compared with the controls, there was a significant decrease in the serum glucose levels of treatments exposed to 1.0 mg/L suspensions of γ-Fe_2O_3 NPs at 30th day ($p < 0.05$), while serum glucose levels of treatments exposed to 1.0 mg/L of α-Fe_2O_3 NPs increased during the elimination period ($p<0.05$). Increasing serum glucose level is indicative of the release of catecholamines and glucocorticoids from adrenal tissues of the fish under stressful conditions to cope with insufficient respiratory function (Klaper et al., 2010), while the decrease suggests excess utilization of stored carbohydrates, presumably due to hypoxic conditions, (Shaluei et al., 2013). Similarly, Savaranan et al. (2015) observed suppression of blood glucose in Indian major carp exposed to 1 and 25 mg/L suspensions of α-Fe_2O_3 NPs. This effect was attributed to the respiratory disturbances caused by Fe_2O_3 NPs.

Iron concentrations in blood serum of treatments did not show any significant changes in comparison to controls. Obviously, dissolved Fe levels (ca. 4 to 21 μg/L) in the exposure medium were too small to induce any changes on high Fe levels in fish's blood that ranged between 28 to 65 mg/L throughout the exposure period. This result therefore could be ascribed to that ingested Fe_2O_3 NPs or aggregates were continually trapped in the organs. Increasing serum Fe levels during elimination period (90th day) supports this explanation as it reflects the mobilization of trapped Fe_2O_3 aggregates from the organs gradually into the fish's blood. Disturbances in GOT, GPT, ALP, and LDH activities are indicators of toxic conditions when these enzymes penetrate to the blood due to cytolyses of liver (Kaya et al., 2014). There were transient increases in GOT, GPT and LDH levels during the course of the exposure for both α-Fe_2O_3 and γ-Fe_2O_3 NPs, while ALP values remained relatively unaffected. Similarly, Lee et al. (2014) reported transient increases in GOT and GPT values of carp during chronic exposure to ZnO NPs, while serum ALP and LDH did not change. Exposure to more toxic AgNPs in contrast increased GOT, GPT, ALP, and LDH levels significantly in rainbow trout (Imani et al., 2014).

4.6. Immune parameters

The RBA levels were not overtly increased or suppressed under the exposure conditions in this study. There was an increase for the treatments exposed to 0.1 mg/L colloids of γ-Fe_2O_3 NPs on the 60th day (Fig. 3), but this was not consistent with the other concentration regimes and thus could be regarded as transient effect. However, lysozyme activity (LA) was found to be suppressed significantly in comparison to controls on the 60th day ($p < 0.05$),

suggesting an immunosuppressive effects of α-Fe_2O_3 and γ-F_2O_3 NPs on *O. niloticus*. In addition, there was a concentration-dependent increase in the myeloperoxidase (MPO) enzyme levels on the 60th day for α-Fe_2O_3 NPs treatments indicating increased oxidative stress ($p < 0.05$). The MPO activity was also enhanced but only marginally in the γ-F_2O_3 NPs treatments ($p \geq 0.05$). Though differences in LA and MPO activities could be associated with morphological differences, overall these results demonstrate immunotoxicity of Fe_2O_3 NPs even at environmentally feasible concentrations. Similar adverse effects were observed from ZnO NPs on *O. niloticus (*Kaya et al., 2016*)*. While RBA levels were increased by small ZnO NPs, large ZnO NPs showed suppressive effects. In addition, large ZnO NPs suppressed LA levels more significantly than small size ZnO NPs. In another study, Cu NPs were found to reduce intestinal lysozyme activity in juvenile estuary cod (*Epinephelus coioides*) more than $CuSO_4$ (Wang et al., 2015).

5. Conclusions

This study is among the first detailing the morphological differences on accumulation, physiological distribution, elimination of waterborne α-Fe_2O_3 and γ-F_2O_3 NPs on tilapia, as well as the impact of chronic exposure on hemolytic and immune system of the fish. Overall, exposure to aqueous suspensions of γ-F_2O_3 NPs resulted in significantly greater accumulation in the organs of tilapia. Spleen possessed the highest accumulation followed by intestine, kidney and liver. Despite rapid accumulation, elimination was slow from spleen that retained a significant amount of ingested α-Fe_2O_3 NPs. On the other hand, γ-Fe_2O_3 NPs were mostly retained in the liver. These effects could be related with morphological differences, but further investigations are needed. The results provide evidence that Fe_2O_3 NPs induce physiological disturbances on serum biochemical markers and Fe levels of tilapia as well as exhibit immunosuppressive and stimulatory effects under chronic exposure. These findings clearly show that further investigations should be conducted to understand the sensitivity of aquatic species to toxicological effects of Fe_2O_3 NPs and other nanomaterials that are considered to be environmentally benign.

Acknowledgements

This work has been supported by the Scientific Research Project Fund of Tunceli University under the project number MFTUB013-17. Partial support has been provided by NIH-RCMI Program at Jackson State University (Grant No: G12RR013459). The views expressed herein are those of the authors and do not necessarily represent the official views of the funding agencies and any of their sub agencies. The authors also thank anonymous reviewers for their valuable comments that helped tremendously in refining the manuscript and improving clarity of discussion.

References

Arslan Z, Ates M, McDuffy W, Agachan MS, Farah IO, Yu WW, Bednar AJ. Probing metabolic stability of CdSe nanoparticles: Alkaline extraction of free cadmium from liver and kidney samples of rats exposed to CdSe nanoparticles. Journal of Hazardous Materials. 2011; 192:192–199. [PubMed: 21700388]

Ates M, Daniels D, Arslan Z, Farah IO, Rivera HR. Comparative evaluation of impact of Zn and ZnO nanoparticles on brine shrimp (*Artemia salina*) larvae: effects of particle size and solubility on toxicity. Environmental Science: Processes and Impacts. 2013; 15:225–233. [PubMed: 24058731]

Ates M, Dugo MA, Demir V, Arslan Z, Tchounwou PB. Effect of copper oxide nanoparticles to sheephead minnow (*Cyprinodon Variegatus*) at different salinities. Digest Journal of Nanomaterial and Biostructures. 2014; 9:369–377.

Ates M, Daniels J, Arslan Z, Farah IO. Comparative study of accumulation, toxicity and trophic transfer of CuO and ZnO nanoparticles through waterborne and dietary exposure of goldfish (*Carassius auratus*). Environmental Toxicology. 2015; 30:119–128. [PubMed: 24860999]

Bakardjieva S, Stengl V, Subrt J, Houskova V, Kalenda P. Photocatalytic efficiency of iron oxides: Degradation of 4-chlorophenol. Journal of Physics and Chemistry of Solids. 2007; 68:721–724.

Bombin S, LeFebvre M, Sherwood J, Xu Y, Bao Y, Ramonell KM. Developmental and reproductive effects of iron oxide nanoparticles in *Arabidopsis thaliana*. International Journal of Molecular Sciences. 2015; 16:24174–24193. [PubMed: 26473847]

Boyle D, A. Al-Bairuty GA, Ramsden CS, Sloman KA, Theodore B, Henry TB, Richard D, Handy RD. Subtle alterations in swimming speed distributions of rainbow trout exposed to titanium dioxide nanoparticles are associated with gill rather than brain injury. Aquatic Toxicology. 2013a; 126:116–127. [PubMed: 23178178]

Boyle D, Al-Bairuty GA, Henry TB, Handy RD. Critical comparison of intravenous injection of TiO_2 nanoparticles with waterborne and dietary exposures concludes minimal environmentally-relevant toxicity in juvenile rainbow trout *Oncorhynchus mykiss*. Environmental Pollution. 2013b; 182:70–79. [PubMed: 23896679]

Diana V, Bossolasco P, Moscatelli D, Silani V, Cova L. Dose dependent side effect of superparamagnetic iron oxide nanoparticle labeling on cell motility in two fetal stem cell populations. PLOS One. 2013; 8:e78435. [PubMed: 24244310]

Dreher KL. Health and environmental impact of nanotechnology: Toxicological assessment of manufactured nanoparticles. Toxicological Sciences. 2004; 77:3–5. [PubMed: 14756123]

Ebrahiminezhad A, Rasoul-Amini S, Kouhpayeh A, Davaran S, Barar J, Ghasemi Y. Impacts of amine functionalized iron oxide nanoparticles on HepG2 cell line. Current Nanoscience. 2015; 11:113–119.

Espenes A, Press CM, Dannevig BH, Landsverk T. Immune-complex trapping in the splenic ellipsoids of rainbow trout (*Oncorhynchus mykiss*). Cell Tissue Research. 1995; 282:41–48. [PubMed: 8581925]

Grover VA, Hu J, Engates KE, Shipley HJ. Adsorption and desorption of bivalent metals to hematite nanoparticles. Environmental Toxicology and Chemistry. 2012; 31:86–92. [PubMed: 21994178]

Guivar JAR, Martinéz AI, Anaya AO, Valldares LS, Félix LL, Dominguez AB. Structural and magnetic properties of monophasic maghemite (γ-Fe_2O_3) nanocrystalline powder. Advance Nanoparticles. 2014; 3:114–121.

Gupta AK, Gupta M. Synthesis and surface engineering of iron oxide nanoparticles for biomedical applications. Biomaterials. 2005; 26:3995–4021. [PubMed: 15626447]

Handy RD, Cornelis G, Fernandes T, Tsyusko O, Decho A, Sabo-Attwood T, Metcalfe C, Steevens JA, Klaine SJ, Koelmans AA, Horne N. Ecotoxicity test methods for engineered nanomaterials: practical experiences and recommendations from the bench. Environmental Toxicology and Chemistry. 2012; 31:15e31. [PubMed: 22002667]

Hao L, Chen L, Hao J, Zhong N. Bioaccumulation and sub-acute toxicity of zinc oxide nanoparticles in juvenile carp (*Cyprinus carpio*): a comparative study with its bulk counterparts. Ecotoxicology and Environmental Safety. 2013; 91:52–60. [PubMed: 23375439]

Hu J, Wang DM, Wang JT, Wang JM. Bioaccumulation of Fe_2O_3 (magnetic) nanoparticles in *Ceriodaphnia dubia*. Environmental Pollution. 2012; 162:216–222. [PubMed: 22243867]

Huber DL. Synthesis, properties, and applications of iron nanoparticles. Small. 2005; 1:482–501. [PubMed: 17193474]

Imani M, Halimi M, Khara H. Effects of silver nanoparticles (AgNPs) on hematological parameters of rainbow trout, *Oncorhynchus mykiss*. Comparative Clinical Pathology. 2014; 24:491–495.

Ito A, Shinkai M, Honda H, Kobayashi T. Medical application of functionalized magnetic nanoparticles. Journal of Bioscience and Bioengineering. 2005; 100:1–11. [PubMed: 16233845]

Karn B, Kuiken T, Otto M. Nanotechnology and *in situ* remediation: A review of the benefits and potential risks. Environmental Health Perspectives. 2009; 117:1823–1831.

Kaya H, Çelik EŞ, Yılmaz S, Tulgar A, Akbulut M, Demir N. Hematological, serum biochemical, and immunological responses in common carp (*Cyprinus carpio*) exposed to phosalone. Comparative Clinical Pathology. 2014; 24:497–507.

Kaya H, Aydın F, Gurkan M, Yılmaz S, Mehmet Ates M, Demir V, Arslan Z. Effects of zinc oxide nanoparticles on bioaccumulation and oxidative stress in different organs of tilapia (*Oreochromis niloticus*). Environmental Toxicology and Pharmacology. 2015; 40:936–947. [PubMed: 26513690]

Kaya H, Aydın F, Gürkan M, Yılmaz S, Ates M, Demir V, Arslan Z. A comparative toxicity study between small and large size zinc oxide nanoparticles in tilapia (*Oreochromis niloticus*): Organ pathologies, osmoregulatory responses and immunological parameters. Chemosphere. 2016; 144:571–582. [PubMed: 26398925]

Khedr MH, Halim KSA, Soliman NK. Synthesis and photocatalytic activity of nano-sized iron oxides. Materials Letters. 2009; 63:598–601.

Klaper R, Arndt D, Setyowati K, Chen J, Goetz F. Functionalization impacts the effects of carbon nanotubes on the immune system of rainbow trout, *Oncorhynchus mykiss*. Aquatic Toxicology. 2010; 100:211–217. [PubMed: 20732719]

Klebanoff, SJ. Oxygen metabolites from phagocytes. In: Gallin, IM.; Goldstein, JI.; Snyderman, MD., editors. Inflammation: Basic Principles and Clinical Correlates. Raven Press; New York: 1992. p. 391-444.

Ladhar C, Geffroy B, Cambier S, Treguer-Delapierre M, Durand E, Brèthes D, Bourdineaud JP. Impact of dietary cadmium sulphide nanoparticles on *Danio rerio* zebrafish at very low contamination pressure. Nanotoxicology. 2014; 8:676–68. [PubMed: 23883150]

Lee JW, Kim JE, Shin YJ, Ryu JS, Eom IC, Lee JS, Kim Y, Kim PJ, Choi KH, Lee BC. Serum and ultrastructure responses of common carp (Cyprinus carpio L.) during long-term exposure to zinc oxide nanoparticles. Ecotoxicology and Environmental Safety. 2014; 104:9–17. [PubMed: 24632117]

Mahmoudi M, Laurent S, Shokrgozar MA, Hosseinkhani M. Toxicity evaluations of superparamagnetic iron oxide nanoparticles: cell “vision” versus physicochemical properties of nanoparticles. ACS Nano. 2011; 5:7263–7276. [PubMed: 21838310]

Nations S, Wages M, Canas JE, Maul J, Theodorakis C, Cobb G,P. Acute effects of Fe_2O_3, TiO_2, ZnO and CuO nanomaterials on *Xenopus laevis*. Chemosphere. 2011; 83:1053–1061. [PubMed: 21345480]

Nudo LP, Catap ES. Anti-immunosuppressive effects of *Chromolaena odorata* (Lf.) King and Robinson (*Asteraceae*) leaf extract in Cyclophosphamide-injected Balb/C Mice. Philippine Journal of Science. 2012; 141:35–43.

OECD. Guideline for the Testing of Chemicals. Organisation for Economic Co-operation and Development (OECD); 2004. Part 203

Quade MJ, Roth JA, Rapid A. Direct assay to measure degranulation of bovine neutrophil primary granules. Veterinary Immunology and Immunopathology. 1997; 58:239–248. [PubMed: 9436268]

Ramsden CS, Smith TJ, Shaw BJ, Handy RD. Dietary exposure to titanium dioxide nanoparticles in rainbow trout, (*Oncorhynchus mykiss*): no effect on growth, but subtle biochemical disturbances in the brain. Ecotoxicology. 2009; 18:939–951. [PubMed: 19590957]

Remya AS, Ramesh M, Saravanan M, Poopal RM, Bharathi S, Nataraj D. Iron oxide nanoparticles to an Indian major carp, Labeo rohita: Impacts on hematology, ionoregulation and gill Na^+/K^+ ATPase activity. Journal of King Saud University Science. 2015; 27:151–160.

Saravanan M, Suganya R, Ramesh M, Poopal RK, Gopalan N, Ponpandian N. Iron oxide nanoparticles induced alterations in haematological, biochemical and ionoregulatory responses of an Indian major carp *Labeo rohita*. Journal of Nanoparticle Research. 2015; 17:274.

Sanchez A, Recillas S, Font X, Casals E, Gonzalez E, Puntes V. Ecotoxicity of, and remediation with, engineered inorganic nanoparticles in the environment. Trends in Analytical Chemistry. 2011; 30:507–516.

Scown TM, Van Aerle R, Tyler CR. Review: Do engineered nanoparticles pose a significant threat to the aquatic environment? Critical Reviews in Toxicology. 2010; 40:653–670. [PubMed: 20662713]

Shaw BJ, Al-Bairuty G, Handy RD. Effects of waterborne copper nanoparticles and copper sulphate on rainbow trout, (*Oncorhynchus mykiss*): physiology and accumulation. Aquatic Toxicology. 2012; 116-117:90–101. [PubMed: 22480992]

Shen Y, Huang Z, Liu X, Qian J, Xu J, Yang X, Sun A, Ge J. Iron-induced myocardial injury: an alarming side effect of super paramagnetic iron oxide nanoparticles. Journal of Cellular and Molecular Medicine. 2015; 19:2032–2035. [PubMed: 26041641]

Shipley HJ, Engates KE, Guettner AM. Study of iron oxide nanoparticles in soil for remediation of arsenic. Journal of Nanoparticle Research. 2011; 13:2387–2397.

Soenen SJ, De Cuyper M. Assessing iron oxide nanoparticle toxicity in vitro: current status and future prospects. Nanomedicine. 2010; 5:1261–1275. [PubMed: 21039201]

Stasiak SA, Baumann PC. Neutrophil activity as a potential bioindicator for contaminant analysis. Fish & Shellfish Immunology. 1996; 6:537–539.

Sun TY, Gottschalk F, Hungerbühler K, Nowack B. Comprehensive probabilistic modelling of environmental emissions of engineered nanomaterials. Environmental Pollution. 2014; 185:69–76. [PubMed: 24220022]

Wang T, Long X, Liu Z, Cheng Y, Yan S. Effect of copper nanoparticles and copper sulphate on oxidation stress, cell apoptosis and immune responses in the intestines of juvenile Epinephelus coioides. Fish & Shellfish Immunology. 2015; 44:674–682. [PubMed: 25839971]

Winer JL, Kim PE, Law M, Liu CY, Apuzzo MLJ. Visualizing the future: Enhancing neuroimaging with nanotechnology. World Neurosurgery. 2011; 75:626–637. [PubMed: 21704929]

Yılmaz S, Ergün S, Çelik EŞ. Effect of Dietary Spice Supplementations on Welfare Status of Sea Bass, Dicentrarchus labrax L. Proceedings of the National Academy of Sciences, India Section B: Biological Sciences. 2014:1–9.

Yin CY, Minakshi M, Ralph DE, Jiang ZT, Xie Z, Guo H. Hydrothermal synthesis of cubic Fe_2O_3 microparticles using glycine: Surface characterization, reaction mechanism and electrochemical activity. Journal of Alloys Compounds. 2011; 509:9821–9825.

Yu MK, Jeong YY, Park J, Park S, Kim JW, Min JJ, Kim K, Jon S. Drug-loaded superparamagnetic iron oxide nanoparticles for combined cancer imaging and therapy *in vivo*. Angewandte Chemie International Edition. 2008; 47:5362–5365.

Zhao J, Wang ZY, Liu XY, Xie XY, Zhang K, Xing BS. Distribution of CuO nanoparticles in juvenile carps (*Cyprinus carpio*) and their potential toxicity. Journal of Hazardous Materials. 2011; 197:304–310. [PubMed: 22014442]

Zhang Y, Zhu L, Zhou Y, Chen J. Accumulation and elimination of iron oxide nanomaterials in zebrafish (*Danio rerio*) upon chronic aqueous exposure. Journal of Environmental Sciences. 2015; 30:223–230.

Zhu X, Tian S, Cai Z. Toxicity assessment of iron oxide nanoparticles in zebrafish (*Danio rerio*) early life stages. PLoS One. 2012; 7:e46286. [PubMed: 23029464]

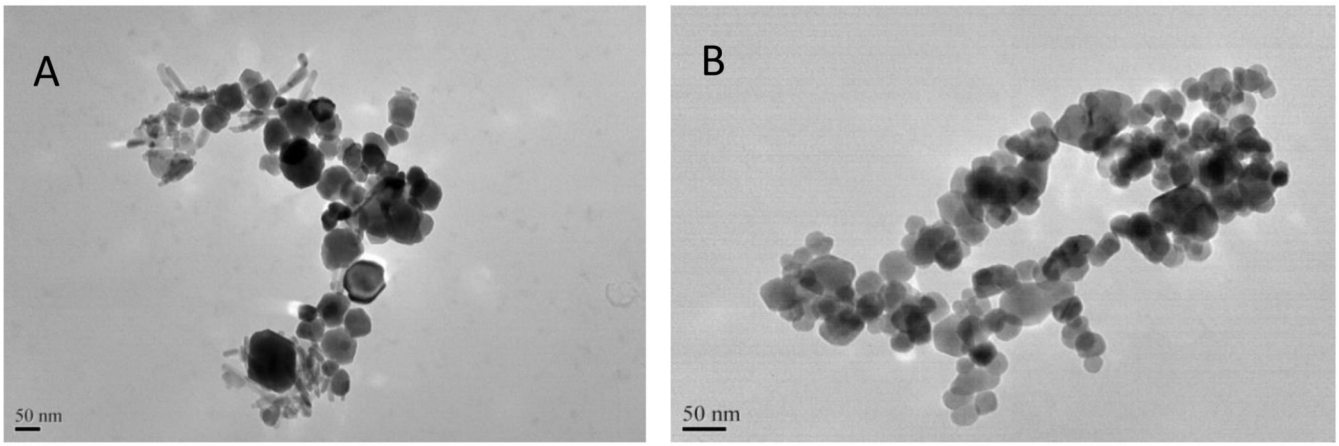

Fig. 1.
TEM images of (A) α-Fe_2O_3 NPs and (B) γ-Fe_2O_3 NPs.

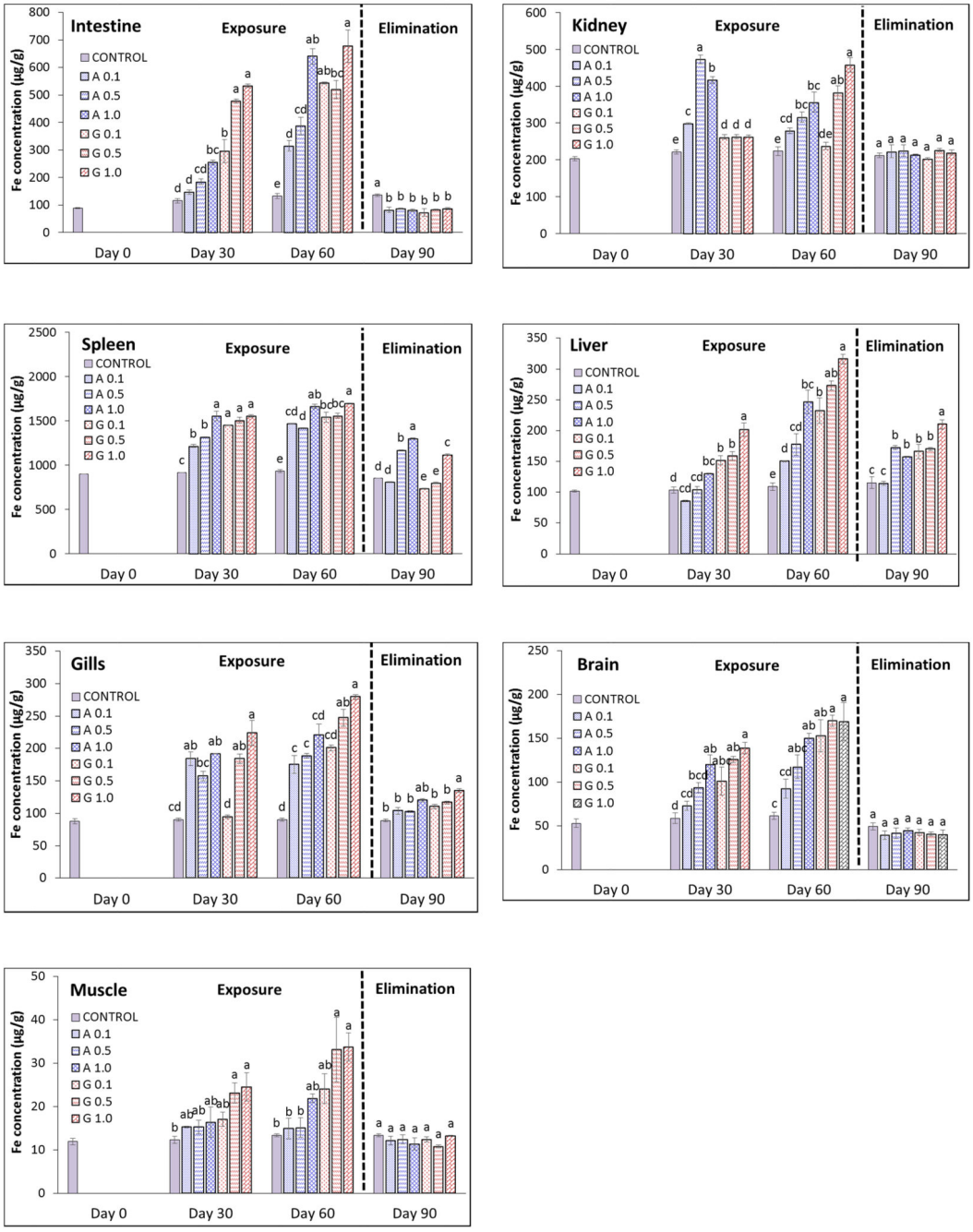

Fig. 2.

Iron concentrations measured in tissues of *Oreochromis niloticus* depicting temporal accumulation and elimination profiles of α-Fe_2O_3 and γ-Fe_2O_3 NPs. A and G in legend denote α-Fe_2O_3 and γ-Fe_2O_3 NPs, respectively, along with exposure concentrations. The mean concentrations denoted with different letters within same exposure period are statistically significant ($p < 0.05$).

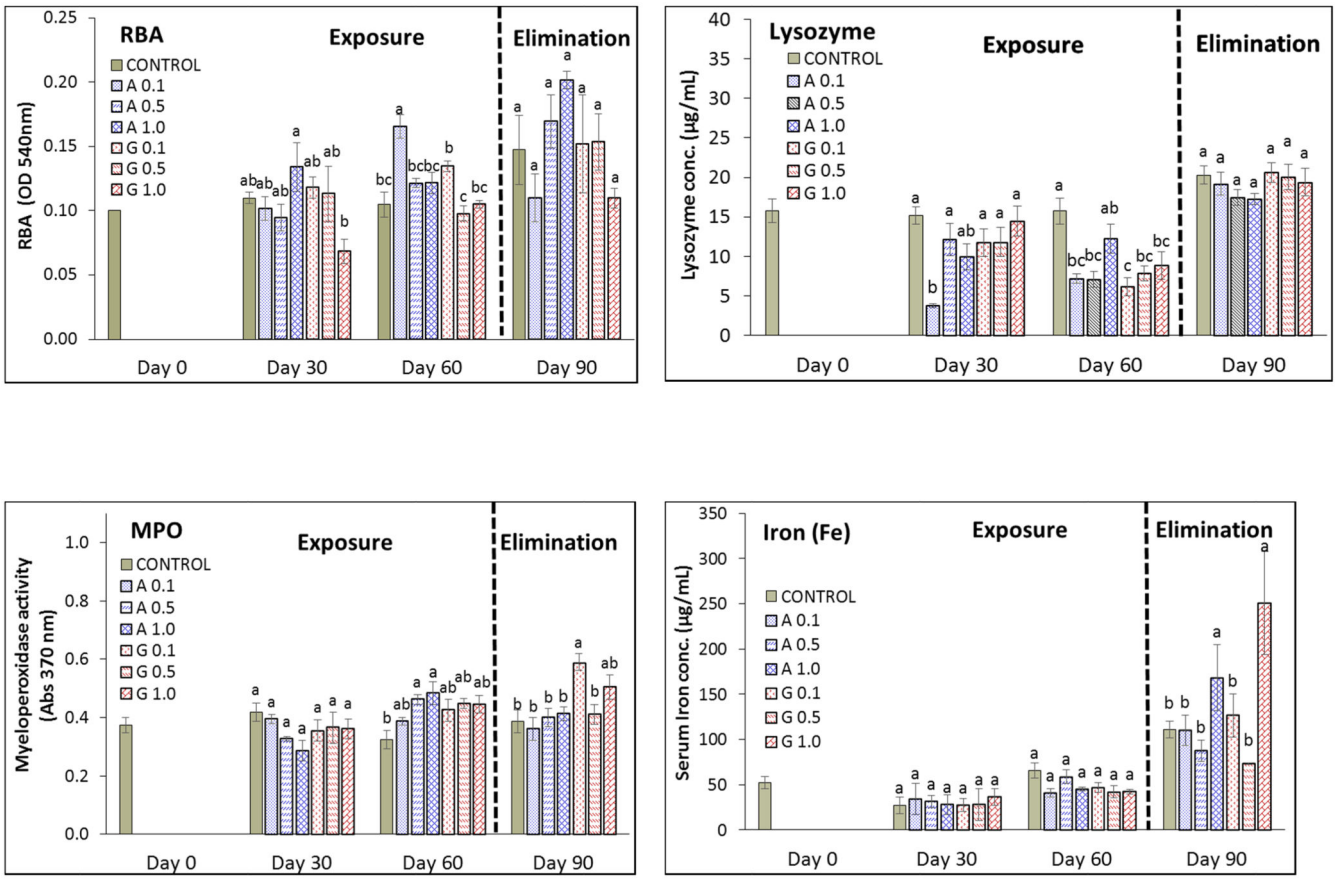

Fig. 3.

Respiratory burst activity (RBA), lysozyme activity (LA), myeloperoxidase activity (MPO) and serum iron (Fe) levels in tilapia (*O. niloticus*) exposed to α-Fe_2O_3 (A) and γ-Fe_2O_3 (G) NPs. A and G in legend denote α-Fe_2O_3 and γ-Fe_2O_3 NPs, respectively, along with exposure concentrations. The mean values denoted with different letters within same exposure period are statistically significant ($p < 0.05$).

Table 1

Experimental design for chronic exposure of tilapia to aqueous suspensions of α-Fe_2O_3 and γ-Fe_2O_3 NPs

	Control	Treatments		
Volume of exposure medium (L)	20	20	20	20
NP concentration (mg/L) *	0 (0)	0.1 (9.2×10^{-4})	0.5 (4.6×10^{-3})	1.0 (9.2×10^{-3})
Duration (day) **	90	90	90	90
Number of fish	15	15	15	15
Recurrence	3	3	3	3

Values in parenthesis are molar concentrations (mM) of AgNP suspensions.

*Concentrations were applied separately for each polymorph of Fe_2O_3 NP.

**Duration reflects 60 days for NP exposure and 30 days for elimination.

Table 2

Effect of chronic exposure to α-Fe_2O_3 (A) and γ-Fe_2O_3 (G) NPs on hematological variables in *O. niloticus* on day 0, 30, 60 and 90. The mean concentrations denoted with different letters within same exposure period are statistically different ($p < 0.05$)

	Groups	WBC counts (10^3/mm^3)	RBC counts (10^6/mm^3)	HGB (g/dL)	HCT (%)
Initial		12.4 ± 0.33	2.54 ± 0.11	10.3 ± 0.43	27.6 ± 1.3
30th day	**Control**	9.98 ± 0.11	2.70 ± 0.13	9.14 ± 0.49	25.6 ± 1.4
	A 0.1	9.93 ± 0.24	2.75 ± 0.05	9.96 ± 0.16	26.9 ± 0.55
	A 0.5	10.2 ± 0.18	2.64 ± 0.10	9.58 ± 0.35	25.2 ± 1.1
	A 1.0	9.63 ± 0.17	2.52 ± 0.06	9.20 ± 0.19	24.3 ± 0.62
	G 0.1	10.0 ± 0.35	2.65 ± 0.14	9.42 ± 0.47	25.5 ± 1.3
	G 0.5	9.36 ± 0.39	2.49 ± 0.13	8.78 ± 0.49	23.9 ± 1.3
	G 1.0	9.58 ± 0.20	2.45 ± 0.11	9.02 ± 0.55	23.6 ± 1.3
60th day	**Control**	12.7 ± 0.13	2.57 ± 0.06	12.6 ± 0.14	43.6 ± 1.3
	A 0.1	12.6 ± 0.48	2.63 ± 0.10	13.1 ± 0.71	44.7 ± 1.8
	A 0.5	13.2 ± 0.33	2.77 ± 0.07	13.2 ± 0.54	48.2 ± 1.5
	A 1.0	12.5 ± 0.32	2.66 ± 0.10	12.9 ± 0.70	45.5 ± 2.1
	G 0.1	12.2 ± 0.39	2.46 ± 0.11	12.4 ± 0.56	41.5 ± 2.1
	G 0.5	13.3 ± 0.42	2.64 ± 0.11	14.8 ± 1.0	45.4 ± 2.3
	G 1.0	12.7 ± 0.46	2.59 ± 0.10	13.2 ± 0.27	46.2 ± 1.4
Elimination (90th day)	**Control**	11.5 ± 0.91^{ab}	2.52 ± 0.10	11.5 ± 0.32	44.8 ± 0.95
	A 0.1	11.2 ± 0.85^{ab}	2.27 ± 0.08	10.3 ± 0.41	40.7 ± 0.94
	A 0.5	11.8 ± 1.0^{ab}	2.45 ± 0.08	11.0 ± 0.39	42.8 ± 0.98
	A 1.0	9.56 ± 1.3^{b}	2.26 ± 0.12	10.4 ± 0.46	41.5 ± 1.3
	G 0.1	11.6 ± 0.87^{ab}	2.60 ± 0.11	11.4 ± 0.28	44.3 ± 1.1
	G 0.5	9.94 ± 0.61^{b}	2.51 ± 0.10	10.9 ± 0.35	43.3 ± 1.1
	G 1.0	14.5 ± 0.69^{a}	2.60 ± 0.04	12.1 ± 0.21	44.5 ± 0.35

Table 3

Effects of chronic exposure to α- Fe_2O_3 NPs (A) and γ-Fe_2O_3 NPs (G) on serum biochemical variables (glucose (GLU), glutamic oxaloacetic transaminase (GOT), glutamic pyruvic transaminase (GPT), lactate dehydrogenase (LDH) and alkaline phosphatase (ALP) in *O. niloticus* on the 0, 30th, 60th and 90th days. The mean concentrations denoted with different letters within same exposure period are statistically different ($p < 0.05$)

	Groups	GLU (U/L)	GOT (U/L)	GPT (U/L)	LDH (U/L)	ALP (U/L)
Initial		52.4 ± 3.5	37.7 ± 2.7	11.8 ± 0.78	252 ± 16	17.9 ± 1.5
Day 30	**Control**	46.2 ± 1.2^{a}	34.3 ± 4.3^{b}	11.1 ± 1.0^{a}	235 ± 18 ^{a}	18.4 ± 1.8^{ab}
	A 0.1	46.9 ± 2.9^{a}	54.2 ± 5.0^{a}	11.7 ± 0.38^{a}	249 ± 21 ^{a}	17.7 ± 1.3 ^{ab}
	A 0.5	31.8 ± 2.3 ^{ab}	46.3 ± 1.8 ^{ab}	10.7 ± 1.2^{a}	222 ± 2^{a}	21.3 ± 0.95 ^{a}
	A 1.0	35.4 ± 2.3 ^{ab}	46.1 ± 4.5 ^{ab}	9.33 ± 0.83^{a}	212 ± 16 ^{a}	15.9 ± 1.6 ^{ab}
	G 0.1	34.8 ± 2.6 ^{ab}	44.2 ± 4.8 ^{ab}	9.56 ± 0.93^{a}	194 ± 8 ^{a}	16.1 ± 1.3 ^{ab}
	G 0.5	32.3 ± 6.6 ^{ab}	41.3 ± 3.5 ^{ab}	8.32 ± 0.63^{a}	209 ± 18 ^{a}	14.3 ± 0.67 ^{b}
	G 1.0	19.7 ± 3.9 ^{b}	37.5 ± 3.7 ^{ab}	9.88 ± 1.4^{a}	188 ± 22 ^{a}	16.3 ± 1.3^{ab}
Day 60	**Control**	49.5± 5.2 ^{a}	39.3 ± 3.2 ^{b}	8.28 ± 0.82^{b}	185 ± 10 ^{b}	19.8 ± 1.4 ^{a}
	A 0.1	43.5 ± 3.4 ^{a}	45.9 ± 6.2 ^{b}	8.96 ± 0.91^{ab}	240 ± 25 ^{ab}	20.9 ± 2.1 ^{a}
	A 0.5	51.5 ± 4.4 ^{a}	43.2 ± 3.8 ^{b}	12.0 ± 1.3^{ab}	199 ± 18^{b}	24.9 ± 1.6 ^{a}
	A 1.0	45.5 ± 1.6 ^{a}	51.5 ± 3.0 ^{ab}	11.6 ± 1.0^{ab}	195 ± 23^{b}	26.1 ± 1.5 ^{a}
	G 0.1	43.5 ± 1.8^{a}	51.4 ± 5.3 ^{ab}	12.8 ± 0.87^{ab}	221 ± 15^{b}	20.2 ± 1.2 ^{a}
	G 0.5	46.2 ± 2.0 ^{a}	68.8 ± 5.4 ^{a}	13.5 ± 1.4^{a}	214 ± 21^{a}	23.7 ± 1.4 ^{a}
	G 1.0	54.6 ± 6.0 ^{a}	58.1 ± 3.8 ^{ab}	9.36 ± 1.4^{ab}	242 ± 15^{ab}	25.6 ± 1.5 ^{a}
Day 90 (Elimination)	**Control**	42.1 ± 2.8 ^{bc}	51.2 ± 3.7 ^{a}	8.33 ± 0.77^{a}	225 ± 15^{a}	23.3 ± 1.8 ^{a}
	A 0.1	51.1 ± 4.5 ^{abc}	57.7 ± 6.7 ^{a}	11.4 ± 2.1^{a}	236 ± 19^{a}	26.4 ± 1.3 ^{a}
	A 0.5	56.8 ± 3.4^{ab}	53.9 ± 4.2 ^{a}	9.46 ± 1.1^{a}	279 ± 21^{a}	22.1 ± 1.8 ^{a}
	A 1.0	63.3 ± 5.4 ^{a}	52.1 ± 5.4 ^{a}	8.96 ± 0.79^{a}	216 ± 17^{a}	21.1 ± 2.7 ^{a}
	G 0.1	40.5 ± 3.6^{bc}	65.7 ± 5.8 ^{a}	10.1 ± 1.03^{a}	259 ± 30^{a}	24.0 ± 1.7 ^{a}
	G 0.5	32.3 ± 4.8^{c}	53.8 ± 3.3 ^{a}	8.90 ± 0.85^{a}	232 ± 11^{a}	22.0 ± 2.0 ^{a}
	G 1.0	57.8 ± 6.5^{ab}	57.1 ± 2.5 ^{a}	8.54 ± 0.28^{a}	264 ± 5^{a}	23.0 ± 1.0 ^{a}